MAUSAM, **55**, 1 (January 2004), 155-176

551.501.815 : 551.515.2

An overview of first Doppler Weather Radar inducted in the cyclone detection network of India Meteorological Department

P. RAJESH RAO

India Meteorological Department, New Delhi, 110 003, India

and

S. KALYANA SUNDARAM, S. B. THAMPI, R. SURESH and J. P. GUPTA

Cyclone Detection Radar Station, IMD, Chennai - 600 001, India

(*Received 12 September 2002, Modified 28 May 2003*)

सार – भारत मौसम विज्ञान विभाग चक्रवातों, गर्ज भरे तूफानों, हवा के तेज झोकें आदि जैसी भीषण मौसम परिघटनाओं का पता लगाने एवं इनका अध्ययन करने और उपरितन वायु पवन प्रोफाइल का पता लगाने के लिए रेडारों के विस्तृत संजाल का रखरखाव करता है। मौसम रेडार तकनीक के क्षेत्र में तीव्र गति से हो रहे विकास के साथ कदम मिलाते हुए भारत मौसम विज्ञान विभाग धीरे–धीरे अपने पुराने रेडारों के स्थान पर नए डिजिटल रेडार लगा रहा है जिनमें से कुछ रेडार डॉपलर क्षमता वाले भी है। हाल ही में, चेन्नै में पुराने एनालॉग एस. बैंड रेडार के स्थान पर भारत मौसम विज्ञान विभाग के चक्रवात संसूचन रेडार (सी.डी.आर.) संजाल में एस. बैंड डॉपलर मौसम रेडार (डी. डब्ल्यू. आर.) सम्मिलित किया गया और इसने 21 फरवरी 2002 से कार्य करना आरम्भ कर दिया है। इस शोध पत्र में रेडार के हार्डवेयर और सॉफटवेयर दोनों की मुख्य विशेषताओं पर विचार विमर्श किया गया है।

ABSTRACT. India Meteorological Department (IMD) maintains a wide network of radars for the detection and study of severe weather phenomena like cyclones, thunderstorms, gust front etc. and for deriving upper air wind profile. To keep pace with the fast developments in the field of weather radar technology, IMD is gradually replacing its conventional radars with digital radars, a few of them with Doppler capabilities. An S-band Doppler Weather Radar (DWR) has been inducted into India Meteorological Department's (IMD) Cyclone Detection Radar (CDR) network recently at Chennai as a replacement to the outlived analogue S-band radar and is declared operational from 21 February 2002. Salient features, both hardware and software, of the radar are discussed in this article.

Key words – Doppler Weather Radar, Digital receiver, Signal processing, Radar products, Aviation.

1. Introduction

Conventional weather radars are analogue devices giving qualitative measurements of weather echoes. However, quantitative measurements by digitizing the echo information have been made possible from these analogue radars in the late 1950s by adding add-on modules such as digital video integrator and processors. Fast developments in digital techniques have been adopted in radar technology to make precise quantitative measurements possible and to incorporate computer control and monitoring systems in radars. Though digitization has enabled more operational convenience and brought out versatile products from weather radars, estimation of radar reflectivity factor and position of hydrometeors in weather systems continued to be the basic principle of weather radars, till the introduction of Doppler shift principles in 1950s into the radar technology. Modern weather radars are invariably digital radars and most of them are with Doppler capability. Doppler Weather Radars (DWR) are capable of probing internal motions of hydrometeors within a sample volume and hence to derive velocity and turbulence information in addition to intensity, rain rate, vertical extent, drop size distribution etc. of weather systems around the radar-site. This capability adds a new dimension to cyclone tracking and forecasting task. Now with DWR it is possible to determine the maximum velocity prevailing inside a cyclonic storm precisely and use this additional information in improving the intensity and storm surge predictions which was not possible, hitherto, with the conventional radars. The upgradation of analogue radar network by the DWR network in United States of America under the project NEXRAD (Next Generation Weather Radar) commenced during late 1980s. Though the details of NEXRAD are beyond the scope of this paper and can

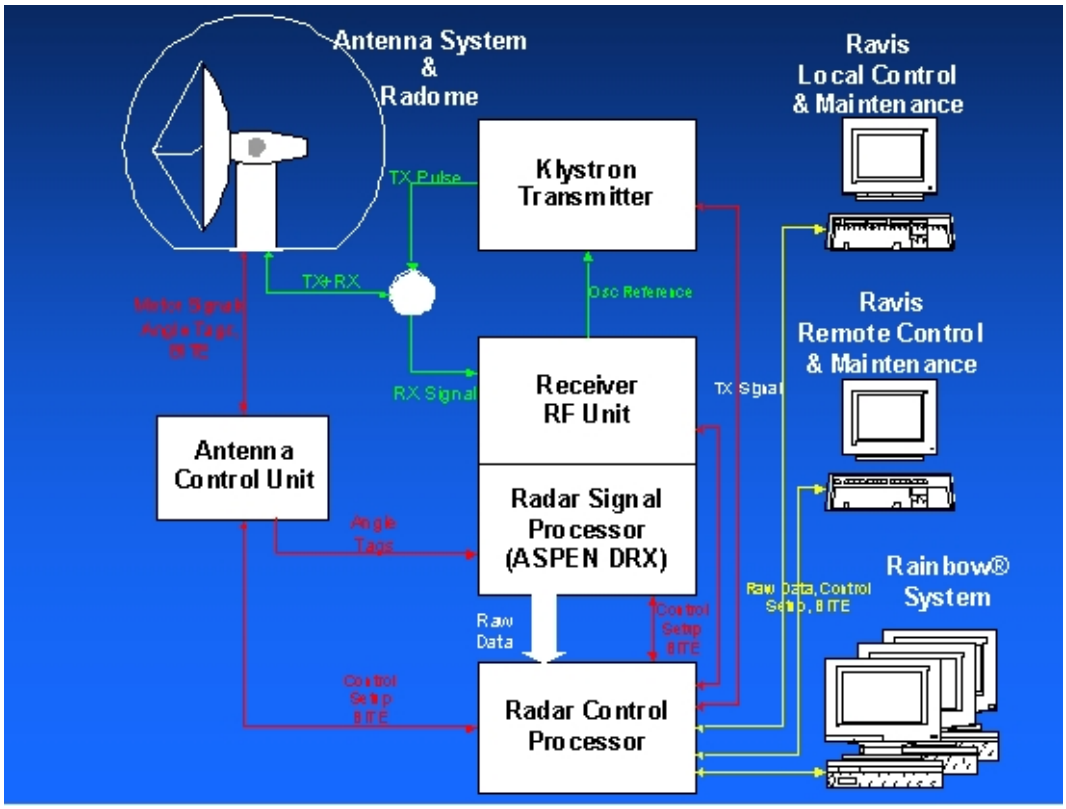

Fig. 1. Doppler Weather Radar system configuration

be seen elsewhere, interested readers may see Heiss *et al*. (1990), Bear (1991), Crum and Alberty (1993) and Klazura and Imy (1993) for a quick reference.

In India, as part of replacing the analogue radars by digital radars/DWRs, an analogue S-band radar which had outlived its life has been replaced by a new Doppler radar with klystron transmitter, solid state modulator and digital receiver operating on S-band (2875 MHz) with linear polarization and 1° beamwidth during October 2001 - February 2002. The system has been put into operational use with effect from 20 February 2002. This article aims at keeping the reader informed about the technical and scientific details / specifications of the DWR installed at Chennai. The system was supplied by M/s Gematronik GmbH, Neuss, Germany on turnkey basis. The system configuration is given in Fig. 1. Hardware details of DWR, Chennai have been summarized at Annexure I. Details and functionalities of the Transmitter, Receiver, Antenna and Radome may be seen in any standard book on Radar technology such as Skolnik (1970), Atlas (1990), Doviak and Zrnic (1993) and Rinehart (1999). Some of the sub-systems especially about the digital receiver and its associated functions, built in test equipment (BITE) are discussed, in brief, in the following sections for the benefit of the readers since the DWR is the first of its kind in India.

2. Facilities available in DWR, Chennai

2.1. *Frequency agility*

The receiver is specially equipped with frequency agility (FA) and phase modulation features. FA is a technique by which the efficiency of time integration is increased. Faster sampling rate results in lack of fresh information from consecutive samples. By changing the transmit frequency by 1 MHz each for four consecutive pulses (2875, 2876, 2877 and 2878 MHz) and cyclically sequencing further pulses in that order, decorrelation of scattered distribution in echo volume faced by the radar pulse is artificially made faster and a better result in time averaging is achieved. The change in frequency is effected by selecting one of the four crystal oscillators in the second LO unit operating at frequencies separated by 1 MHz (465, 466, 477, 478 MHz) as second LO in sequence. However, in this mode velocity measurements are not possible.

Phase modulation is a technique used to distinguish between echoes from one pulse and its previous pulses

reaching the receiver simultaneously. Rather it is used to filter out multi-trip echoes and for recovering at least second trip echoes for display in their right position. Emitter Coupled Logic (ECL) clock from the Digital Receiver (DRX) gives the necessary phase coding and the Digital filters in the Radar Signal Processor (RSP) retrieves the second trip echoes. For a detailed description on signal processing techniques see, for example, Keeler and Passarelli (1990) and Doviak and Zrnic (1993).

2.2. *ASPEN DRX*

The Advanced Signal Processing Environment Digital Receiver (ASPEN DRX) is the intelligent link between the radar echo acquisition hardware consisting of the analogue receiver part of the receiver RXS-1500, the klystron transmitter, the antenna system, and the radar product generation and processing system. This powerful stand-alone system receives radar IF signals from the analogue receiver, commands and operational parameters from the Radar Control Processor (RCP) and provides in return the required signal parameters, headers, and states for each Doppler and non-Doppler data sets. The ASPEN DRX is a digital receiver/radar signal processor combination using powerful application specific integrated circuits, Analogue to Digital Converters (ADCs) and floating point Digital Signal Processor (DSP) chips. By digitizing the IF signal immediately after the radar mixer, and performing all normal receiver functions in software rather than hardware, it provides improved performance, wider dynamic range, higher linearity, increased amplitude stability, and better clutter rejection than conventional receivers. At the same time it eliminates many of the analogue subsystems like linear and log IF amplifiers, Coherent oscillator, AFC unit, demodulator etc. Software programming permits complete flexibility in IF pass band shaping, base band video filtering, Stable Local Oscillator (STALO) frequency control and various trigger and reference signal generation. Provision for continuous monitoring of transmitter power, frequency and spectrum is inbuilt in digital receiver (DRX). Excellent linearity of the ASPEN DRX makes calibration possible using a single point power output for a known input.

2.3. *DRX functions*

The heart of the ASPEN signal processor is a set of Analogue device Super Harvard ARChitecture (SHARC) signal processors. It is booted from a 2 MB flash Programmable Read Only Memory (PROM) holding the firmware. Communication to outside world is through six link ports and two high-speed serial ports. For hardware debugging a parallel port is also provided. All other activities of the ASPEN processor is controlled *via* the external SHARC data and address buses. A 40.0 MHz master clock drives all functions including Analogue to Digital (A/D) conversion DSP clocking and general logic clocking. All system timing signals requiring synchronization are generated by a master timing state machine having 32-bit width and 256 k word-depth. As the state machine is driven by a 40 MHz clock (25 ns state width), the longest possible pulse repetition time (PRT) is 256*1024* 25 ns = 6.55 ms equivalent to pulse repetition frequency (PRF) = 152.6 Hz or maximum range of 982.5 km, well beyond the operationally useful range of weather radar. The basic triggers are generated in the DRX and sent to the Trigger Transfer Unit (TTU).

There are three analogue IF input to the digital receiver, each designed to process IF signals at 10 MHz centre frequency at different power levels having a dynamic range of –85 dBm to – 5dBm. The High (HI) channel processes the lower part of the system dynamic range and the Low (LO) channel processes the higher part of the system dynamic range. The transmitter (TX) channel processes the IF signal from the TX sample circuit. The receiver output signal is directly connected to HI channel and a 25 dB attenuated tapping is fed to LO channel. All input signals pass through a relay switch, to allow calibration using the internal IF calibration unit, then the signal is amplified and filtered prior to A/D conversion. The signal amplification is designed to preserve high linearity and low distortion for the nominal dynamic range of each channel.

The three identical analogue channels are digitized by three identical 12-bit, 40 MHz A/D converters. The output of the HI and LO channels converters are sent to IF digital filters for further processing. The HI channel ADC output is also sent to the dynamic range logic for input selection. The TX ADC output is stored in the TX FIFO (first in first out) for use by the DSP for transmitter frequency and phase referencing. The IF digital filters process the digitized IF input to them from ADC and derive the in phase (I) and quadrature (Q) components (I/Q demodulation). The output of the digital filter is digitised according to the temporal resolution required by the current range-gate width. The 16-bit digitised I/Q data is stored in the I/Q data memory.

DSPs process the raw I/Q data as per values set for different parameters and perform phase and amplitude correction, clutter filtering, covariance computation and produce normalized results. These normalized results are tagged with angle information, headers and given out as a data set. Covariance computation is based on pulse pair processing. This includes computation of the autocorrelation functions R0, R1 and R2 at lag 0, 1 and 2 respectively. Since the signal is complex linear in nature,

intensity estimation consists simply of integrating the power in the linear channel (I^2+Q^2) over range and azimuth. The resulting power estimate is corrected for system noise, for atmospheric attenuation and for transmitter power variations. The signal processing of the linear channel ends with the estimation of reflectivity, the mean radial velocity and the velocity spectrum width.

The ASPEN processors provide selectable frequency-domain clutter filtering in the Doppler mode. The I and Q channel filters are implemented digitally as three-pole elliptic Infinite Impulse Response(IIR) filter with rejection depth of 30 to 50 dB. The filters are available in 16 different widths including a zero-width all pass filter. For the operating frequency 2875 MHz and PRF range of 250-1200 Hz, the notch widths of the clutter filters vary between 0.0 and 8.92 ms^{-1}. Doppler clutter filters remove almost completely those echoes whose velocities are within the notch width of the clutter filter selected. For example, clutter filter No. 5 with 600 PRF has a notch width of $\pm 1 ms^{-1}$. In this case, echoes having a radial velocity within ± 1 ms^{-1} will be removed. This facility is very useful in filtering out ground clutters which are more predominant during anomalous propagation (AP) conditions. However, in some cases we may lose a few precipitation echoes too in this process. ASPEN processors include a speckle-removing algorithm. Speckles are isolated echoes surrounded by 'no data' values. They may be due to noise spikes, reflections from planes, clutter or at times may be due to isolated rain cell. Speckle removing algorithm is a user selectable option which when left enabled would keep the radar displays free of random point targets. Provision for applying signal quality thresholds is available. The Signal Quality Index (SQI) is the normalised magnitude of the auto correlation function at lag 1 (*i.e.*) SQI = |R1| / R0. SQI is a measure of the linear channel coherency. Bins not meeting the thresholds are discarded. Another threshold is the clutter-to-signal-threshold, which computes the clutter to signal ratio and discards bins below a user-set value.

2.4. *Radar calibration*

As any other measurement device, DWR needs to be calibrated to ensure reliability of results. Calibration in this context can be defined loosely as the measurement of the gains and losses of the radar, which finally leads to the radar constant. The calibration is done in three phases. They are (*i*) initial or basic calibration (*ii*) automatic online calibration and (*iii*) manual offline maintenance calibration. The initial calibration is performed during the final acceptance tests by measuring the complete system parameters that are part of the radar equation or using vendor data, where a measurement is not possible. Transmitter power, waveguide losses, receiver losses, antenna parameters, radome losses, and wave length and pulse width are the measurable parameters leading to the radar constant. The radar constant is saved within the configuration files for the ASPEN DRX RSP.

The online calibration controls at frequent intervals the injection and processing of calibration signals at range gates, which are usually beyond that part of atmosphere having weather data (at an elevation of 60°). Operation of the radar is not interrupted and no data are lost. For calibration purpose, ASPEN DRX incorporates the following facilities: (*i*) Intensity Test Signal Generator (TSG) for single point calibration (*ii*) Noise source for noise figure measurements (*iii*) Power monitor for reverse power at the klystron output (*iv*) TX channel for forward power monitoring at klystron output and (*v*) Zero check for noise level of ADC. The minimum digitally detectable signal is around –114 dBm in long pulse (LP) mode and –113 dBm in short pulse (SP) mode. The dynamic range over which the receiver response is linear is about 97 dB for LP and 96 dB for SP.

Voltage Standing Wave Ratio (VSWR) is computed from the forward and reverse power values measured. VSWR is a measure of the antenna-waveguide system health. Noise figure is calculated by monitoring the received noise power in return of the noise injected at proper intervals. Noise figure is used to subtract noise-power from the total received power. Zero check is performed by keeping the antenna in 60 degree and shutting down all inputs to the receiver. The ADC output in that condition is subtracted from the ADC output in other times in order to linearise the receiver response curve. Receiver gain is measured using the internal test signal generator (TSG) at specific level (single point calibration) along with zero check, at frequent intervals and the values incorporated into the radar constant. Manual offline maintenance calibrations are to be performed during annual preventive maintenance activity or after exchange of subsystem parts in addition to the automatic online measurements. Receiver linearity and dynamic range measurements can be performed manually using internal TSG at an antenna elevation of 60°. The internal TSG is to be calibrated once in two or three years by a certified measurement authority and the results to be updated in radar control processor (RCP) for future use. The IF gain of the receiver, TX output power, frequency etc. can also be measured using external signal generator, oscilloscope, power meter and frequency meter to ensure proper functioning of the system and for troubleshooting purpose.

2.5. *Built-in test equipment (BITE)*

The purpose of the BITE is the verification of the system performance. The BITE system monitors the

electrical and mechanical functions of all subsystems, performs the system calibration, detects faults and isolates faulty components, initiates protective measures to save critical component from conditions arising out of fault in other parts (*e.g.* switching off the radiation in case of fault in the antenna drive system) and assists in off-line testing and fault isolation for maintenance. The BITE is not realized by a dedicated physical unit but is integrated in the radar hardware and software consisting of a network of sensors distributed in the hardware, a test signal generator and a noise source, firmware and software for BITE control, logical inference tasks and test algorithms. Active sensors stimulate the device under test and acquire response while passive sensors monitor the performance of the devices. The sensors are controlled by the subsystem programmable logic controller (PLC) or another dedicated control processor. Stimulus signals for the actors are generated by the corresponding subsystem PLC. The results of the checks are sent *via* PROcess FIeld BUS (PROFIBUS) network to the radar control processor (RCP). This information enables localization of the fault. A report about the detected malfunction and its most likely cause is sent to the requesting terminal. If a major fault is detected, which causes the malfunction of the complete subsystem the related subsystem is shutdown to protect it from further damage. For faults, which do not pose any threat to the radar system components, the BITE will send a report containing description to the operator.

2.6. *Data processing, product generation and archival system*

The data processing and product generation and archival tasks are performed by a dedicated software named RAINBOW running on a SUN SOLARIS workstation. Rainbow provides platform for designing scans, planning scan schedules, generating various products using the data received from the radar and for archiving the data for future use. It is also capable of taking over control of the radar and for processing the BITE and status information received from the radar. Radar Control Processor acts as the interface between the ASPEN DRX and the RAINBOW Workstation. The connection is implemented in the form of 10 Mbps Ethernet hardware and TCP/IP protocol. This architecture provides a high degree of flexibility for integrating various outside sensors like rain gauges and data sets like satellite products into the rainbow products. Apart from the main workstation there is a standby workstation normally used for raw-data processing and archival purposes, which can be easily configured to take over the radar control and supervision from the main workstation in case the latter develops some problem. Depending on the weather situation, a 500 km scan of 1000 range bins with 12 elevations may occupy between 2 and 4.5 Mbytes for each of three basic data, *viz*., radar reflectivity, radial velocity and velocity spectrum width. If the antenna scan rate is 3 rotations per minute, then in a day on an average about 1600 Mbytes data is possible from continuous scanning which may be compressed into 550 Mbytes for archival purposes. The base data are archived in 4 mm digital audio tape (DAT) cartridges (12 GB capacity) and also in digital linear tape (DLT) cartridges (40 GB capacity) for off-line processing and for use in research mode.

3. RAINBOW system

The UNIX based RAINBOW system (M/s Gematronik GmbH, Germany) consists of a number of processes. The main rainbow modules are (*i*) Radar Manager, (*ii*) Supervisor Manager, (*iii*) Product Generation Processes, (*iv*) Database and Archival Manager and (*v*) Display Managers.

3.1. *Radar Manager*

Full control of the radar is performed with the Radar Manager. Data acquisition modes and parameters are defined in scan definition files (SDF) whereas the scan schedule and the list of products [as defined in the product definition files (PDF)] to be generated from each set of data acquired are defined in the schedule worksheet. Most of the parameters can be optimised by changing the default values by an authorized supervisor to suit the need of the hour. Scans can be categorized as azimuthal scan (0 – 360° at a fixed elevation) or elevation scan (varying elevation angles at fixed azimuth) or volume scan (antenna rotating 0 – 360° with varying elevations). The speed of the antenna can be varied from one rotation per minute (rpm) to 6 rpm. The data quality is better with lower rpm since it enhances the number of samples considered for deriving the three basic data mentioned in section 2.6. SDFs are defined in such a way that maximum data is collected in each azimuthal and elevation rotation of the antenna taking into account of the beam width and ensuring data quality without much redundancy (overlapping) between two successive elevations. Schedules can be run in either immediate or cyclic loop modes. In cyclic loop mode, the processes of radar control, data acquisition, product generation, generation of warning alarms, and archival are performed automatically and completely unattended. A typical scheduler containing different scans adopted by DWR, Chennai is furnished as Annexure II.

3.2. *Supervisor Manager*

In contrast to the Radar Manager, whose tasks are related to controlling radar operation and product

generation, the tasks of the supervisor manager are related to the administration of the local host computer and the rainbow network. System messages concerning the file system or the network are displayed in the message window. The current BITE status of the radar and its processors is available on every workstation or terminal in the network. Errors and or messages are stored into log files, which can be used to monitor the system activities and performance level. Supervisor manager process alone can perform local shutdown of Rainbow.

3.3. *Product Generation Processes*

All radar products are derived from corrected volume raw data in reflectivity, mean velocity, and spectral width. Some of the corrective algorithms, which enhance the reflectivity and Doppler data quality, are applied in real time at the radar signal processor. Other algorithms like clutter map correction, rainfall rate correction, bright-band correction are applied to the raw data by the product processor. Most of the products are finally displayed in the Cartesian coordinate system in a planar form. The raw data resulting from the scans are collected and stored initially in the memory of the radar control processor with the range resolution selectable by the user (N*150 m). After the raw data set is completed, it is transported to the product-processing task. After this, the radar control processor is free again to collect new raw data while the radar product generation processor generates the products. The raw data are further on projected from the raw polar volume representation into a Cartesian 2D, vertical cross section, horizontal 2D etc. user products with the specified resolution. The conversion from polar to Cartesian coordinates requires interpolation in elevation and azimuth. For each cell or pixel of the Cartesian product, the interpolated value is calculated from the closest neighbours in the polar volume. Most of the products derived from the volume raw data use earth curvature correction for height calculation. The propagation and refraction of the radar beam in the atmosphere are taken into account by applying an effective earth radius, which is 4/3 times the real earth radius. Product generation process also performs 2D clutter correction for all reflectivity and rainfall products. For this, a data file archived during clear weather condition (precipitation echo free) is used to correct the actual data. The clutter reflectivity data are subtracted in linear form from the actually received reflectivity set in the corresponding polar volume.

3.4. *Database and Archival Manager*

The product archival is controlled by the archival manager which is located in the main and display workstations. Database consists of temporary and archive

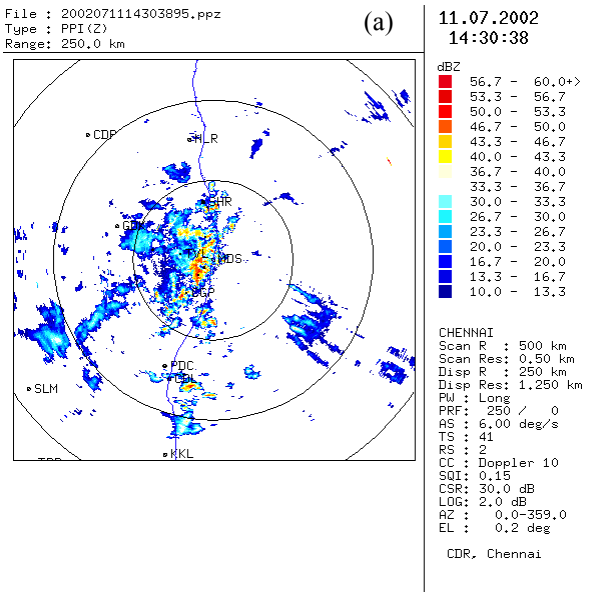

Fig. 2(a). Plan Position Indicator display of logarithmic radar reflectivity factor (dBZ)

sections. The temporary section is working in a FIFO (first in first out) manner. Into this FIFO, a configurable number of products for each type may be stored immediately. Typically 100 products per product-type are stored. This FIFO is accessible by the user at each individual workstation for fast recovery of products and sequences. Into the archive section of the database, user selected products may be stored permanently either automatically or interactively. The product to be stored is chosen according to product-type and storage time interval.

3.5. *Display Managers*

A number of Display Manager modules perform the display of products and all other information at the workstations. Each individual Display Manager performs all local product image processing functions like animation, overlay etc. The Display Managers as well handles superimposition of overlay of multiple optional data sources like other radar data, satellite data etc. The display window provides tools such as Zoom, colour palette choice, Data level distinction with different colours, Choice of radar reflectivity – rain rate conversion parameters and precipitation class, Animation, Overlay (landscape, text, contours, maps etc)., Geographical orientation (altitude, longitude, latitude, distance and angle from radar) or other mouse pointer defined orientation, Interactive cross-section, interactive tracking, System Information (Status information, error messages, audio alarms), utility for converting rainbow product to GIF images etc.

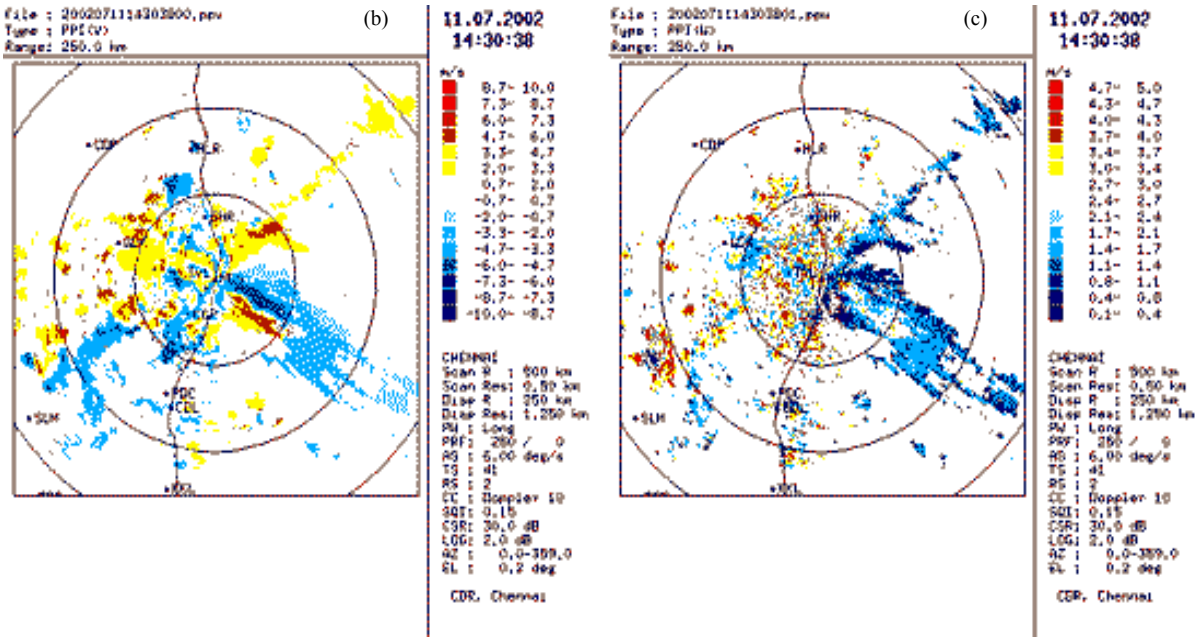

Figs. 2(b&c). Plan Position Indicator display of (b) radial velocity and (c) spectrum width

4. Rainbow products

Rainbow products can be broadly divided into base products, extended products, hydrological products, windshear products, warning and tracking products, phenomena detection and aviation products.

4.1. *Base products*

(a) *Plan Position Indicator (PPI)*

This is the most commonly used type of product display in conventional radar to display the radar reflectivity factor. It gives an overall picture of weather around in a constant elevation surface. However, in the PC based radars colour coding of the radar reflectivity factor helps the user to have a quick glance of the weather. Higher the reflectivity implies higher the rain rate provided the reflectivity is measured from weather echoes and not from the ground clutter. Fig. 2(a) displays a typical PPI of the radar reflectivity. In the case of Doppler weather radars, the PPI type display is used to display the logarithmic reflectivity (dBZ, hereafter called as Z), rainfall rate (R), radial velocity (V), and velocity spectrum width (W) of a polar azimuth scan at a fixed elevation angle. Figs. 2(b&c) depict a sample PPI display of radial velocity and spectrum width. Radial velocity information is conventionally displayed as "cool" colours (blue and green) to indicate the approaching velocity (towards radar) and "warm" colours (yellow and red) to indicate receding (away from the radar). The velocity spectrum width is a measure of turbulence since higher the spectrum width higher the velocity spread within the sample volume. Spectrum width of more than 4 ms^{-1} is considered as moderate turbulence (Rinehart, 1999).

(b) *Range Height Indicator (RHI)*

Display of Z, R, V and W data of a polar elevation scans at fixed azimuth angle. This is also one of the common types of display in conventional radars. This gives the vertical cross section of weather cells in the prescribed azimuth direction.

(c) *Constant Altitude PPI (CAPPI) and Pseudo CAPPI*

Display of Z, R, V and W generated by a polar volume scan at number of elevation angles converted to earth curvature corrected Cartesian coordinate system. It displays echoes at a fixed height above ground at each point. It is also known as horizontal cut. Depending on the height selected it displays all points for which data is available from the selected volume data set. As the range increases, radar beam may be above the height selected under CAPPI and hence the display is limited to that area wherein the radar beam cuts the height selected. Due to this limitation, echoes are seen in an annular region around the radar. However, in order to know the immediate extension of any particular height selected, the

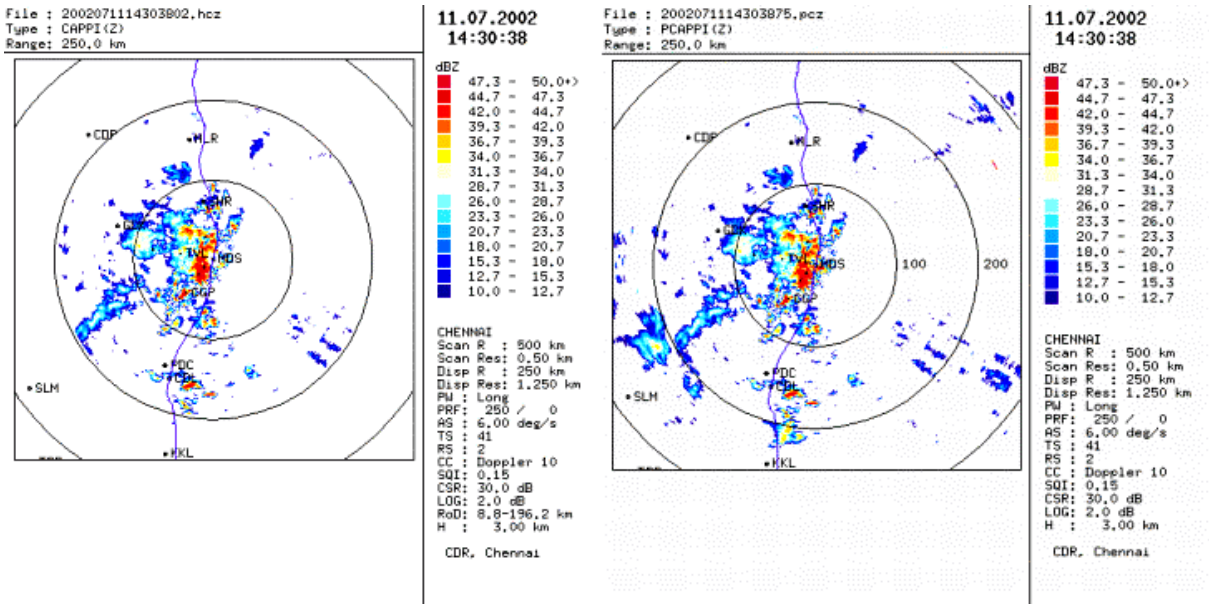

Fig. 3. CAPPI and Pseudo CAPPI plot

data from the beam just above the height selected is plotted in the area wherein there is no data in the CAPPI layer. This product is called Pseudo CAPPI display. As can be seen from Fig. 3, for a 3 km constant altitude the range of CAPPI is restricted between 8.8 and 196.2 km from the radar whereas in the case of Pseudo CAPPI the range from the radar is not at all restricted since at the farther range the data from the elevation just above the altitude selected by the user is displayed in this product. The user should understand the difference between CAPPI and Pseudo CAPPI especially when interpreting the data from the farther range to the fact that the data has been filled from the next available height and not pertaining to the altitude chosen by him or displayed in the product.

(d) *Vertical cut (VCUT)*

Display of vertical cross section of data through the volume data-set between two arbitrary points positioned under cursor control on the CAPPI or MAX display. Alternatively, the arbitrary points can be defined in a text window as Cartesian coordinates. Vertical cross sections obtained using RHI is having a limitation that one of the points between which the cut is performed is fixed (Radar Centre) whereas in VCUT the cut axis is having the full degree of freedom in XY plane. However RHI products have more data density because the data acquisition is product specific whereas vertical cut (VCUT) products obtained from a general purpose scans have less data

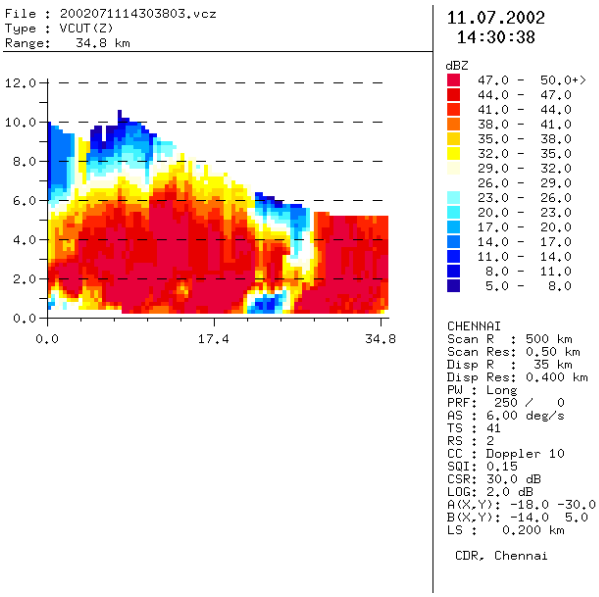

Fig. 4. Vertical cut of reflectivity

density and hence show more staircase effect. Fig. 4 shows the VCUT product. The distance coordinates (km) of the two points *w.r.t* radar in the conventional x-y geometry scale are indicated in the legend.

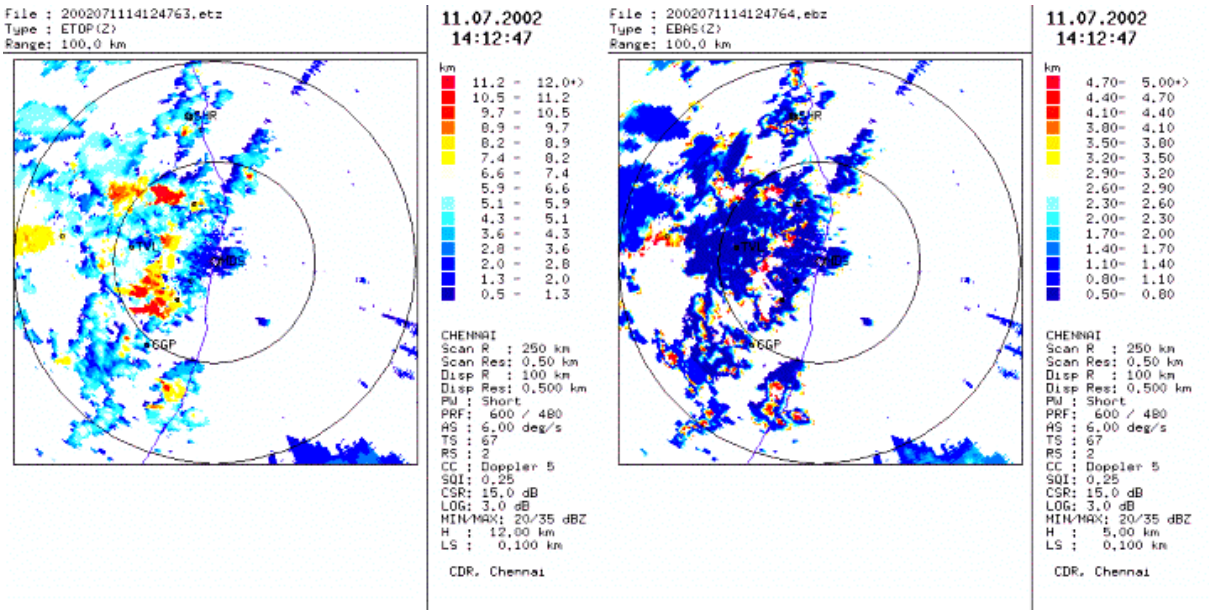

Fig. 5. Plots of Echo top and Echo base

(e) *Echo Top (ETOP) and Echo Base (EBASE)*

The ETOP (EBASE) product displays the height of the upper most (bottom most) occurrence of a user specified range of Z, R data level in the volume hemisphere obtained from a volume scan. A downward (upward) search is performed within the minimum and maximum height specified by the user in the data volume set converted into cylindrical form. The search is performed in vertical tubes whose dimensions decide the horizontal resolution (dx, dy) and the vertical resolution is defined by another parameter called dh. By knowing the height of the upper most (bottom most) occurrence of the specified Z value, one can infer the height of the convective cloud or the vertical stretch of the intense form of precipitation or the possibility of hail stones etc. For ease of visualization, the height is displayed in colour code. Fig. 5 shows a sample plot of ETOP and EBASE.

(f) *Maximum Display (MAX)*

Display of maximum value of Z, R, V and W data generated from a volume scan. At first, the data set is converted into earth curvature corrected Cartesian coordinate form. The search for maximum value is performed in vertical and horizontal tubes whose dimensions decides the product resolution. In the final projected image, each tube is represented by a pixel, which is set to the colour code of the maximum value

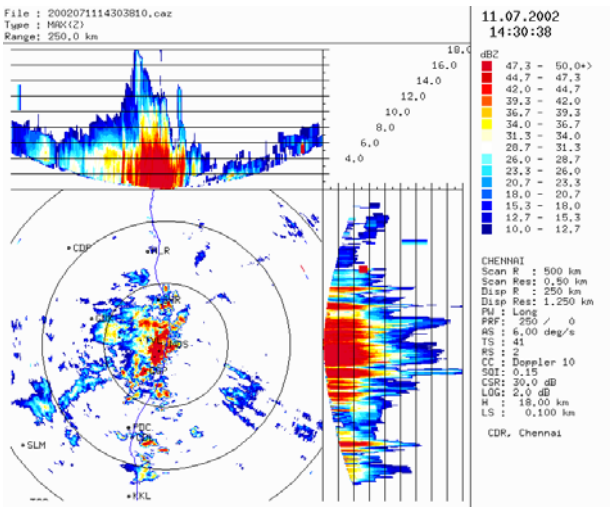

Fig. 6. Max (Z) product display

encountered in the search of that tube. The display (Fig. 6) consists of three images, the vertical maximum projection, north-south maximum projection, and east-west maximum projection.

4.2. *Extended Meteorological products*

(a) *Velocity Azimuth Display (VAD)*

VAD as defined originally (Lhermitte and Atlas, 1961) was to record, when the antenna is rotated in a

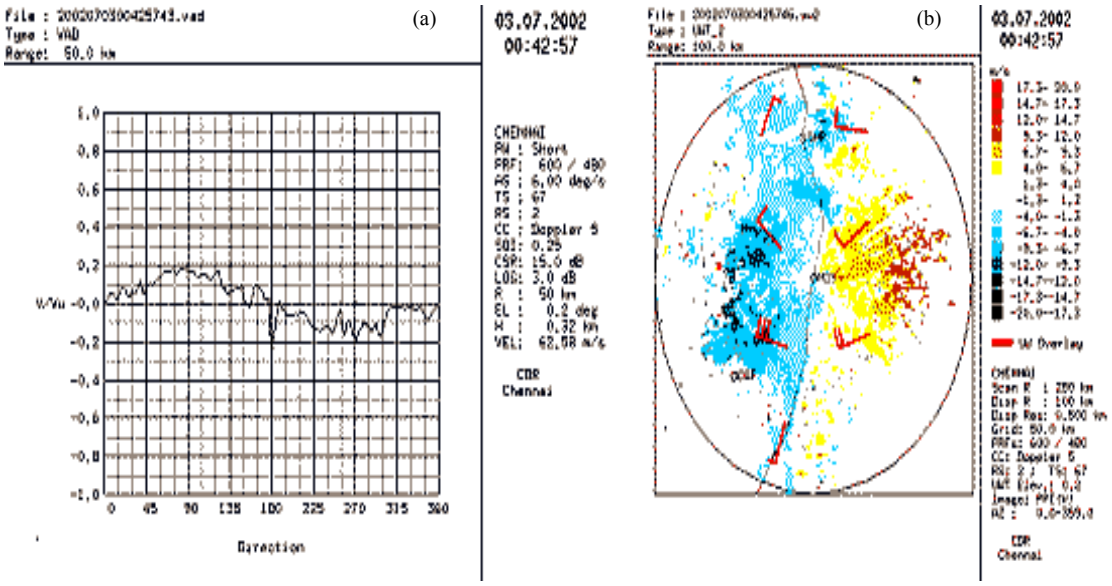

Figs. 7(a&b). Display showing (a) Velocity Azimuth Display (VAD) and (b) Uniform Wind Technique

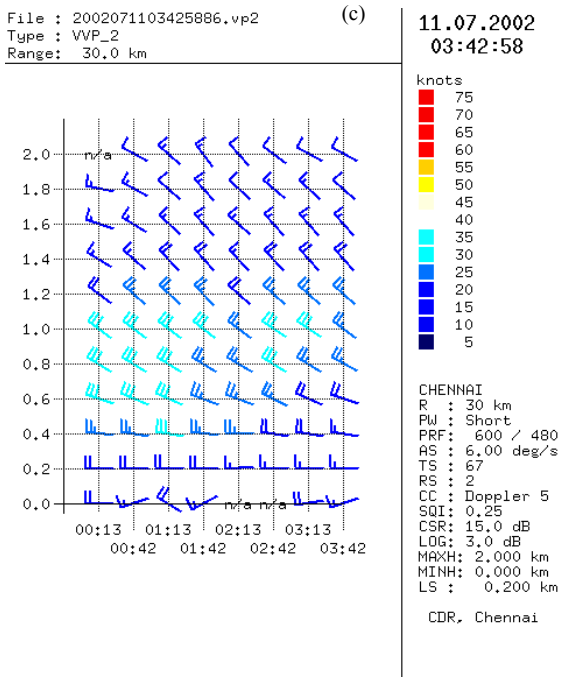

Fig. 7(c). Horizontal wind estimation from radial velocity information by Volume Velocity Processing

circle at constant elevation angle, the radial velocities at a fixed slant range close to the radar site to obtain wind velocity profiles in widespread precipitation. Later this technique was modified by Browning and Wexler (1968) to estimate the kinematics of wind fields such as horizontal wind, divergence and deformation by employing harmonic analysis. However with the modern DWRs, this technique can be used in non-precipitation conditions as well since the modern receivers are quite sensitive to detect clear air returns. A typical plot of

radial velocity against azimuth will look like a sinusoidal curve if wind field is uniform. The horizontal wind vector can be estimated under these assumptions, which may be prevailing only in fair weather and in stable atmospheric conditions. Fig. 7(a) shows the plot of VAD at 0.2° elevation and 50 km range from Chennai DWR. The abscissa is the azimuth angle and the ordinate is the normalized radial velocity (radial velocity divided by the maximum velocity retrievable for that particular scan).

Mathematically, the radial velocity (V) can be expressed as

$$V = V_h \cos\alpha \cos(\beta - \beta_0) - V_f \sin\alpha \quad (1)$$

where V_h and β_o are the horizontal wind speed and direction respectively, V_f is the fall velocity of the particles, α is the antenna elevation angle and β is the azimuth angle. A quick interpretation of the above equation would lead to $V = V_h$ when α is very small and when $\beta = \beta_o$ or $\beta = \beta_o + \Pi$. When the radar beam is pointed towards the prevailing wind direction (upwind) (*i.e.*) when $\beta = \beta_o$, V is maximum – but by convention approaching winds are assigned negative velocities. Hence V is minimum (negative maximum) when the radar beam is pointed upwind. Similarly, when the radar beam is pointed downwind (*i.e.*, when $\beta = \beta_o + \Pi$), V is minimum – but by convention receding winds are assigned positive velocities. Hence V is maximum when the radar beam is pointed downwind. We can approximately estimate the horizontal wind directions prevailing at that elevation/ height by considering the azimuthal angle of upwind as it is or by adding 180° to the downwind. In the example presented here, since some amount of perturbation in the wind field has caused the VAD to be not exactly sinusoidal and the maximum and minimum values are not confined to a single value (point) azimuth, the horizontal wind direction can be any angle between 260 and 270°.

When the prevailing wind is normal to the radar beam, the radial velocity is zero. Hence another way of estimating the wind direction from the display is from the zero radial velocity. To get the prevailing wind, one can add 90° to the azimuth of the zero radial velocity when the change in the display is from +ve to –ve or by subtracting 90° when the change is from –ve to +ve if the display resembles a sinusoidal curve. In the example considered, this method also confirms the variability of the horizontal wind direction between 260 and 270° since the zero radial velocity did not occur at a single point alone.

As regards the speed of the wind, the minimum (or maximum) value displayed in the ordinate has to be multiplied by the maximum velocity that can be measured unambiguously or by unfolding technique. In the current example, since we used dual pulse repetition frequency (PRF) to invoke velocity unfolding technique, a maximum velocity of 62.58 ms^{-1} is possible and hence the approximate wind speed is 12.2 ms^{-1} (= 0.195 * 62.58) or 23 kts. Hence the wind vector at 0.32 km (approximately representing 50 km radius at 0.2^o elevation) around Chennai at 0042 UTC/ 3 July 2002 can be taken as 265/23 kts. The 0000 UTC Rawin sonde observation at 0.348 km was 269/22 kt and the Pilot Balloon observed value at 0.3 km was 270/21 kt. Though the VAD estimated wind vector agrees with that of Rawin sonde and Pilot Balloon observed value in this case (in the almost stable atmospheric condition in the early hours), it should be remembered that VAD may not be valid if the horizontal wind field is not uniform. Such non-uniformity in wind field is not at all uncommon in tropical atmosphere due to high amount of insolation as the day progresses, induced convective currents, topographic and terrain conditions etc. Also the VAD technique is valid only for small elevation angles whether it is during precipitation or in clear air mode. Hence the interpretation requires adequate experience and its utility may be made with a word of caution.

(b) *Uniform Wind Technique (UWT)*

As the name suggests uniform wind field is assumed in this technique. This technique developed by Persson and Andersson (1987) gives a simplified way to ease the interpretation of horizontal fields of measured Doppler velocity. This technique is an extension of methodology adopted by Royal Netherlands Meteorological Institute (KNMI). It is assumed that $V_{ri} = u_{ri} \sin(i) + v_{ri} \cos(i)$ where V_{ri} is the radial velocity and u_{ri} and v_{ri} are the U and V component of the horizontal wind vector at range r and azimuth i. The U and V components of the horizontal wind are estimated using least square regression technique to minimise the function $\sum_i [u_{ri} \sin(i) + v_{ri} \cos(i) - V_{ri}]^2$ for each slant range r. The regression is performed for each cell (any value from 4 to 100 km/cell) defined in the resolution of the grid. Speckles whose departure from the area mean by more than the user defined threshold settings are considered as outliers and are excluded from the computation. The elevation or the height of the underlay product definition file is considered for computing the horizontal wind. The output would be better if the number of regression points are more, obviously. A typical plot of the wind derived at 0.2° elevation at 0042 UTC / 3 July 2002 over an underlay of the corresponding PPI (V) has been displayed as Fig. 7(b). Horizontal winds derived appears to be quite comparable in this uniform flow of wind field. Here also the wind field is assumed to be uniform in the area of analysis for deriving the actual wind from the radial velocity. When

the wind blows in a uniform way without perturbation or turbulence etc (may be possible in stable atmospheric conditions), the estimation of horizontal wind is done. In Fig. 7(b), the underlay is the PPI (V) at 0.2° elevation and the estimated wind is plotted using the conventional wind vector plotting methods. One can see that the prevailing wind on that day was from west to east (approaching velocity in blue colour to receding velocity in red colour) which agrees with the (southwest monsoon) seasonal wind during July over peninsular India. Horizontal wind field derived with a spatial resolution of about 5 × 5 km is displayed in the form of colour coded wind barbs in a PPI type of display at 50 × 50 km grid. Any other product [such as PPI (Z), CAPPI (Z or V)] corresponding to the same time stamp can be selected as an underlay for the UWT product.

(c) *Volume Velocity Processing (VVP)*

The VAD was originally limited to only one elevation angle. If we want to find out the velocity estimations over different heights, then we need to process a volume data comprising the VAD data of various elevation angles. As the name implies this product computes and displays the mean radial velocity at different heights in a cylindrical volume around the radar. The display format is mean radial velocity in colour codes on height over azimuth display. The radius of data volume is to be kept low, typically 20 to 30 km, to have meaningful values. The raw data comes from a volume scan covering sufficient number of elevations to get wind information from the desired upper level at the selected range. The horizontal wind vector and the kinematics of wind field can be derived by adopting suitable algorithms and the display can be in the form of (*i*) a vertical time section of horizontal wind and/or (*ii*) three displays showing height over wind direction, wind speed and horizontal divergence at a particular time. The radial velocity V_r as observed by radar can be written as

$$V_r = u \cos\theta \cos\varphi + v \sin\theta \cos\varphi + w \sin\varphi \qquad (2)$$

where θ and φ are the azimuth and elevation angles. In this algorithm the wind $V = V(u,v,w)$ is assumed to vary linearly in space around its value (u_0 , v_0 , w_0) at a point, usually the radar centre, (x_0 , y_0 , z_0).

(*i.e.*)

$$u = u_0 + u'_x(x - x_0) + u'_y(y - y_0) + u'_z(z - z_0)$$

$$v = v_0 + v'_x(x - x_0) + v'_y(y - y_0) + v'_z(z - z_0)$$

$$w = w_0 + w'_x(x - x_0) + w'_y(y - y_0) + w'_z(z - z_0)$$

By transforming into polar coordinates (R, θ, φ) where R is the radius (slant range in our case) and regrouping we obtain

$$\begin{aligned} V_r = {} & \cos\theta \cos\varphi (u_0 - u'_x x_0 - u'_y y_0 - u'_z z_0) \\ & + \sin\theta \cos\varphi (v_0 - v'_x x_0 - v'_y y_0 - v'_z z_0) \\ & + \sin\varphi (w_0 - w'_x x_0 - w'_y y_0 - w'_z z_0) \\ & + R \cos^2\theta \cos^2\varphi u'_x + R \sin^2\theta \cos^2\varphi v'_y \\ & + R \cos\theta \sin\theta \cos^2\varphi (u'_y + v'_x) + R \sin^2\varphi w'_z \\ & + R \cos\theta \sin\varphi \cos\varphi (u'_z + w'_x) \\ & + R \sin\theta \sin\varphi \cos\varphi (v'_z + w'_y) \end{aligned} \qquad (3)$$

The vorticity derivatives v'_x and u'_y cannot be extracted as they are either summed up with the other unknown quantities such as u_0 and v_0 or summed up together. Thus in order to retrieve u_0 and v_0 in the absence of any additional information, the only possibility is to choose radar as the centre (*i.e.*) $x_0 = 0$ and $y_0 = 0$. When we assume linear approximation (in locally stratiform conditions), w'_y , $w'_x << u'_z$ and v'_z and hence w'_y, w'_x can be neglected. With these assumptions Waldteufel and Corbin (1979) modified the radial velocity term so that the components of radial velocity terms can be retrieved without any contamination by other components. The modified term V_r is

$$\begin{aligned} V_r = {} & \cos\theta \cos\varphi u_0 + \sin\theta \cos\varphi v_0 + \sin\varphi w_0 \\ & + R \cos^2\theta \cos^2\varphi u'_x + R \sin^2\theta \cos^2\varphi v'_y \\ & + R \cos\theta \sin\theta \cos^2\varphi (u'_y + v'_x) \\ & + \sin\varphi (R \sin\varphi - z_0) w'_z \\ & + \cos\theta \cos\varphi (R \sin\varphi - z_0) u'_z \\ & + \sin\theta \cos\varphi (R \sin\varphi - z_0) v'_z \end{aligned} \qquad (4)$$

This formulation can be thought of as an extension of VAD since VAD can be obtained by discriminating those terms which depend on azimuths. Since R and φ are constant and there is no z term in VAD and w'_y, w'_x are very small, the radial velocity term for VAD can now be re-written as

$$\begin{aligned} V_r = {} & \cos\theta \cos\varphi u_0 + \sin\theta \cos\varphi v_0 \\ & + \cos^2\theta (R\cos^2\varphi u'_x + \sin\varphi w_0) \\ & + \sin^2\theta (R \cos^2\varphi v'_y + \sin\varphi w_0) \\ & + \sin\theta \cos\theta R \cos^2\varphi (u'_y + v'_x) \end{aligned} \qquad (5)$$

The computation of horizontal divergence pose serious problem because of the contamination of u'_x and v'_y by the appearance of vertical velocity term w_0. This again re-confirms the applicability of VAD to simply low elevation angles only. The results of attempts made to estimate the vertical component of velocity from radar reflectivity data (mostly from the fall velocity of hydrometeors) are considered far from satisfactory (Battan, 1977). Vertical time section of wind vectors as estimated from VVP is displayed in Fig. 7(c).

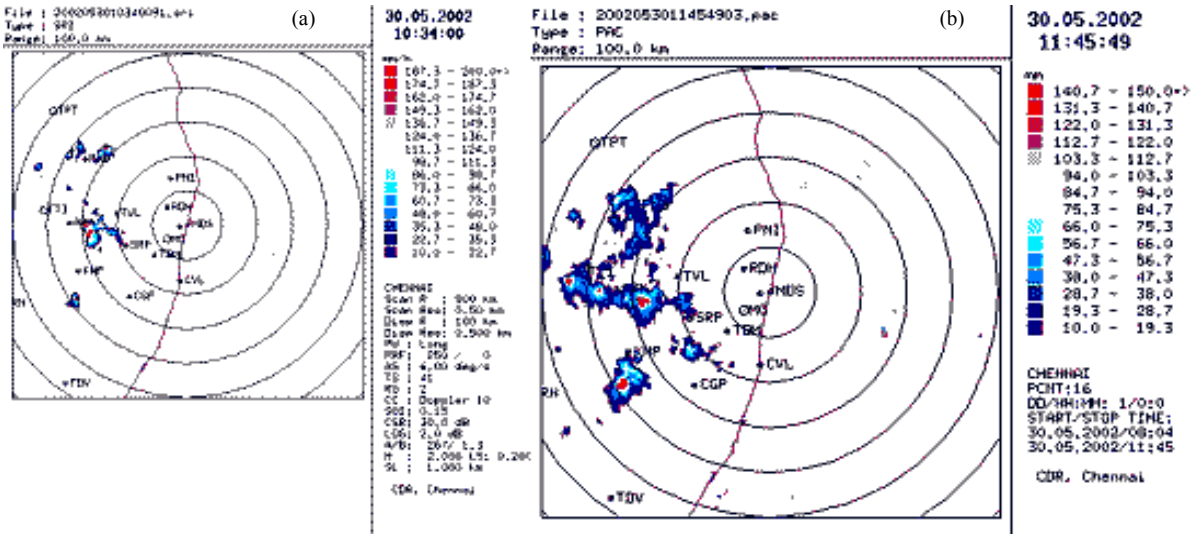

Figs. 8(a&b). Display showing (a) Surface Rainfall Intensity and (b) Precipitation Accumulation products

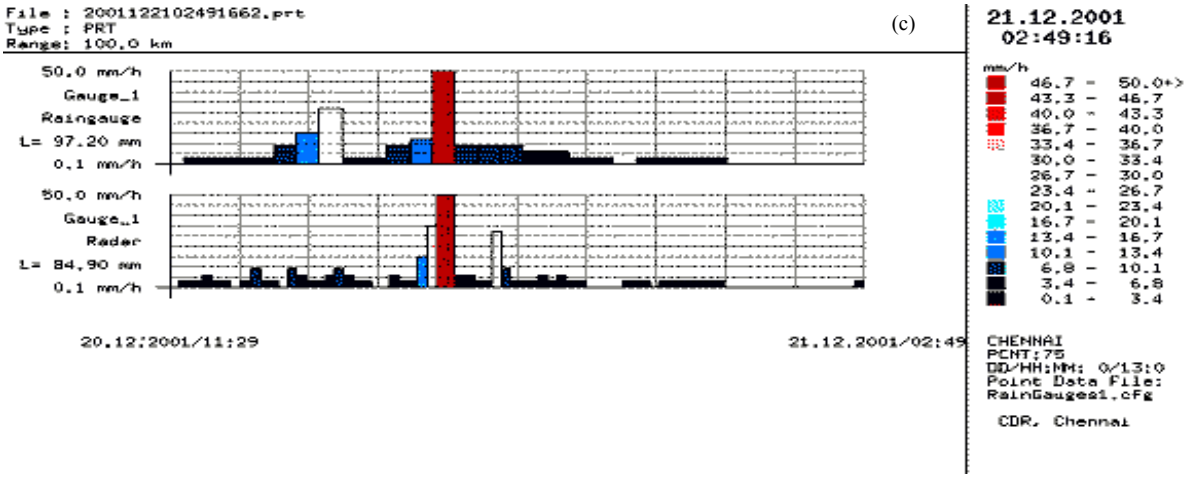

Fig. 8(c). Point Rainfall Total (PRT) display

(d) *Advantages, Demerits and limitations of VVP*

Besides its advantage over the VAD in getting the volume data processed to derive vertical profile of velocity fields, the following are the added advantages of VVP:

(*i*) Horizontal divergence and hence the vertical velocity can be computed using continuity equation

(*ii*) Horizontal wind vector for any elevation / height can be derived easily

(*iii*) Vertical time section of horizontal wind vector is possible

(*iv*) An estimate of fall velocity of hydrometeors can be made from the vertical component of wind that is directly available through this technique.

The following are the demerits and limitations of VVP :

(*i*) The algorithm will work better with a few thousand data samples obtained through faster and quicker volume scans having different elevation angles within a narrow range of altitudes so that computational errors can be minimized by range and time averaging.

(*ii*) Since the algorithm is based on linearity assumptions in stratiform situations, the same may cause serious errors in convective situations.

(*iii*) The accuracy of direct vertical velocity estimation is moderate to poor (Waldteufel and Corbin, 1979) even by combining data from several radars.

(e) *Vertically Integrated Liquid (VIL)*

The reflectivity values observed in a cylindrical volume, the size of which is set by the layer heights and range defined by the user, are converted into mass of liquid water and integrated by suitable algorithms and displayed in a PPI type of display in colour codes. The formula used for converting radar reflectivity factor (z) (unit : mm^6/m^3) into Liquid water content (M) (unit : kg/m^3) is $z = C M^D$ where C and D are to be estimated (Douglas, 1964). The liquid water content is integrated over the user selected atmospheric layer and the product is displayed (unit : kg/m^2 which is equivalent to mm of water). While this product indicates the likelihood of rainfall potential over an area since the radar measures the falling precipitation in a volume, it is mostly used for nowcasting the occurrence of hail. VIL based predictors are most prominent in predicting severe weather events and hail storms and VIL exceeding 50 kg m^{-2} has been identified as one of the potential predictors of severe hail storms (Burgess and Lemon, 1990).

4.3. *Hydrological products*

(a) *Surface Rainfall Intensity (SRI)*

The SRI generates an image of the rainfall intensity in a user selectable surface layer with constant height above ground. A user definable topographical map is used to find the co-ordinates of this surface layer relative to the position of the radar. This map is also used to check for regions, where the user selected surface layer is not accessible to the radar. These parts of the image will be filled with the NO DATA value. Conversion of reflectivity to rain-rate is performed using the well known $Z - R$ relation (Marshall and Palmer, 1948), *viz*., $Z = A*R^b$, where the adaptable parameters 'A' and 'b' vary in space, time (season) and type of precipitation such as convective, stratiform etc. A typical SRI product based on the $Z - R$ relation $Z = 267*R^{1.345}$ is shown in Fig. 8(a).

A network of rain gauges is used to estimate the areal average of rainfall over catchments over unit time and this information is used in operational hydrology for flash flood forecasting. Though the rain gauge measurements of rainfall are adjudged as standard, the accuracy of areal average depends on the spatial variability of rainfall as well as the density of the rain gauges used to estimate the areal average (Huff, 1970). But it may not be practicable to have rain gauges installed too closely, say at least one in 4 × 4 km grid, due to cost factor, upkeep and maintenance aspects. By comparing the reflectivity factor measured by the radar with the rain rate recorded by the surface rain gauges and extending this relationship to a wider area, the radar is able to measure rainfall at tens of thousands of points every minute. However, there are some limitations in these estimates when the distance from the radar is increased (Rinehart, 1999). Combining the accuracy from the surface rain gauge(s) located in the area of interest and the advantage of wider areal coverage from the radar, one can reliably estimate the rain rate.

The rain rate estimation from radar is subjected to possible sources of error such as (*i*) evaporation beneath the radar beam (*ii*) incomplete beam filling (*iii*) reflectivity enhancement by melting layer which is often referred to as the bright band (*iv*) advection of droplets by winds close to the ground which are beneath the lowest beam of the radar (*v*) in-frequent calibration of radar resulting in change in radar constant (*vi*) underestimation in the absence of large droplets in drizzle and orographic enhancement of rain either below the radar beam or blocked by the hills. By choosing Z at a height of 1.0 km a.g.l. the error due to evaporation can be minimized despite the fact that the height so chosen restricts our range of rainrate estimation to 100 km. By applying suitable correction for the bright band (Andrieu and Creutin, 1995), keeping the antenna height well above the possible interference from ground clutter, beam blocking etc., periodical transmitter and receiver calibration and suitable incorporation of radar constant are a few methods adopted in DWR, Chennai to avert errors mentioned above.

(b) *Precipitation Accumulation (PAC)*

The PAC product is a second level product. It takes SRI products of the same type as input. The PAC product accumulates the rainfall rates of the selected SRI product. The timely accumulation is done according to a user-definable time period (look back time). Every time a new

SRI product is generated, the PAC generation starts again. The display shows the colour coded rainfall amount in [mm] for the defined time period. By comparing with the rain gauge data for the same time and area, this product can be used for validating the Z - R relation. Fig. 8(b) displays accumulated radar estimated precipitation from 0804 to 1145 UTC on 30 May 2002. Since a rain gauge samples an area of about 0.05 sq. m. whereas the radar with a typical pulse length of 150 m samples a volume of several hundreds of cubic meters of rain area at 100 km radius, the amount of information received from the radar may be equal to that obtained from a few lakhs of rain gauges installed in the catchments with 150 m grid spacing. Hence, radar estimated rain rate and thereby the accumulated rainfall will be useful as a first hand information to know about the amount of water accumulated over a wider area despite its uncertainties. This information is helpful to work out the level of ground water table, issue of flash flood forecast, plan for irrigation and water supply operation etc. It is desirable to have the rain rate estimated through radars which gives some information – if not most accurate to the operational hydrologists for devising suitable water conservation scheme.

(c) *Precipitation accumulation for longer periods (PAL)*

The PAL product is a third level product. It takes PAC products of the same type as input. The PAL product accumulates the rainfall amounts of the selected PAC product. The timely accumulation is done according to a user-definable time period (look back time). It is more useful for climatological purposes to calculate the monthly, seasonal, annual and even higher order periodicity rainfall totals. Reliability of this product depends much on the continuity in data acquisition for that period. Corresponding to the periods of uninterrupted data acquisition of the order of months and years, this product would be of immense climatological importance.

(d) *Point Rainfall Total (PRT)*

The PRT product allows the comparison of rain intensity obtained from rain gauges with corresponding radar data. Rain gauge measured rain intensity values (mm/h) are displayed in histograms. Radar data from SRI products also contain rain intensity values and are shown in separate histograms. This is a very good tool for fine tuning the Z - R relation parameters. The rain gauge data of IAF, Tambaram have been tabulated from the self recording rain gauge chart for 20-21 December 2001 and the rainfall values were interpolated for 30 minutes duration between 1130 UTC/20 and 0300 UTC of 21 December. These values have been compared with the radar estimated rainfall based on the $Z - R$ relationship as defined by Marshall and Palmer (1948). The coefficients of 'A' and 'b' have been empirically estimated as 267 and 1.345 respectively based on the data from 1 November to 20 December, 2001. Fig. 8(c) shows the PRT display. Though the radar estimated value appears to be comparable to that of the observed rainfall, it requires more data samples to arrive at stable coefficients which are valid for a particular season. More than 60 values of 'A' and 'b' until 1970 have been documented in literature (Battan, 1973). At least thousand sets of values of 'A' and 'b' might have been arrived at, as of now, based on the research work done throughout the world. Since the digital data of reflectivity is available only from 1 November, 2001 at Chennai, further research is being carried out for different seasons with more data.

4.4. *Wind shear Detection products*

(a) *Radial Shear (RDS)*

The RDS product evaluates the derivative of the wind velocity in radial direction. A single plane of constant elevation is taken as input. The product can be generated from a single elevation scan or from a volume scan. In the second case the algorithm uses the next neighbour of the selected elevation for product generation.

(b) *Azimuthal Shear (AZS)*

The AZS product evaluates the derivative of the wind velocity in azimuth direction. A single plane of constant elevation is taken as input. The product can be generated from a single elevation scan or from a volume scan. In the second case the algorithm uses the next neighbour of the selected elevation for product generation.

(c) *Elevation Shear (ELS)*

The ELS product evaluates the absolute change of the wind velocity in elevation direction. Two planes of constant elevation are taken as input. The product can be generated from any multi-elevation scan. The output values are scaled to units of $m\ s^{-1}\ km^{-1}$.

(d) *Radial Azimuthal Shear (RAS)*

The RAS product takes a volume data set or a single elevation data set as input. The change of the wind velocity is calculated in radial and azimuth direction with a least square fit algorithm. Both shear values are added to find the value of the radial azimuth shear. The output values are always positive and scaled to units of $m\ s^{-1}\ km^{-1}$.

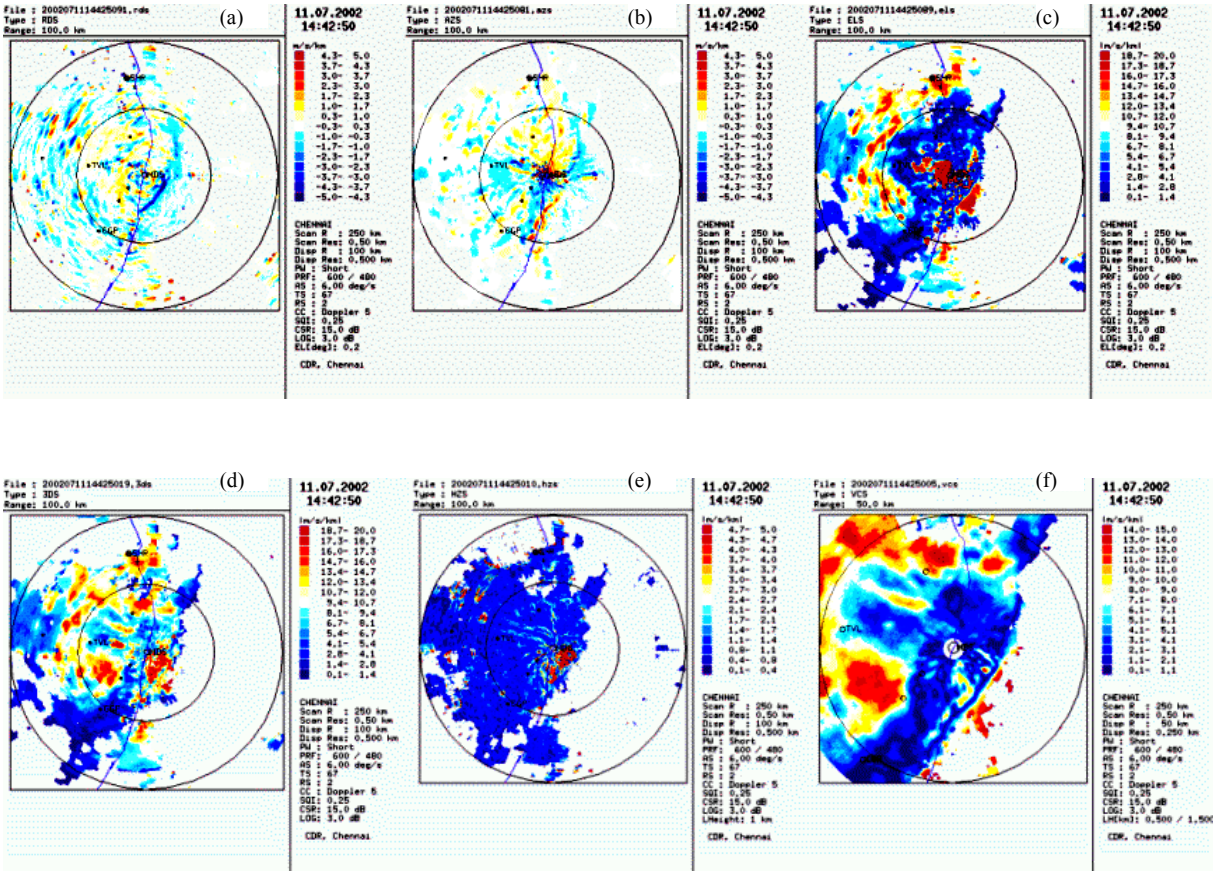

Figs. 9(a-f). Display of (a) radial (b) azimuthal (c) elevation shear (d) three dimensional (e) horizontal and (f) vertical shear

(e) *Radial Elevation Shear (RES)*

The RES product takes a volume data set with at least two elevations as input. The change of the wind velocity is calculated in radial direction and in elevation direction. Both values are added to find the value of the combined shear. The output values are always positive and scaled to units of $m\ s^{-1}\ km^{-1}$.

(f) *Three Dimensional Shear (3DS)*

The 3DS product takes a volume data set with at least two elevations as input. The change of the wind velocity is calculated for each polar bin in radial, azimuth and elevation direction. The three values are added to find the value of the 3D shear. The polar shear volume is converted to a Cartesian volume and a maximum display is generated. The shear values in the final product are always positive and scaled to units of $m\ s^{-1}\ km^{-1}$.

(g) *Horizontal Shear (HZS)*

The HZS product takes a velocity volume data set as input and displays shear values for a single, curvature corrected Cartesian layer. The change of the wind velocity in north-south direction and in east-west direction is calculated and added to find the value of the horizontal shear. The HZS product can be generated from any multiple elevation scan. The output values are scaled to units of $m\ s^{-1}\ km^{-1}$.

(h) *Vertical Shear (VCS)*

The VCS product takes a volume data set as input. Velocity values are calculated for two Cartesian layers. The shear value is defined as the absolute difference of velocities between adjacent Cartesian bins. The output values are always positive and scaled to units of $ms^{-1}\ km^{-1}$. Fig. 9 shows a few shear products.

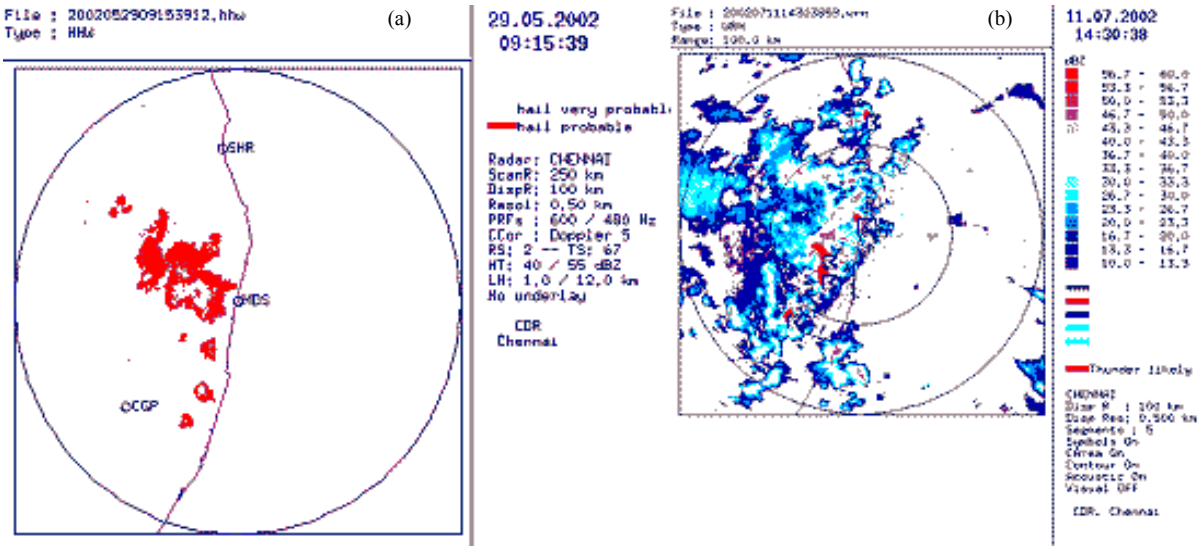

Figs. 10(a&b). Display of (a) Hail warning and (b) warning of severe weather products

4.5. *Warning and forecasting products*

(a) *Hail Warning (HW)*

Climatologically the probability of hail over Chennai is practically nil [India Meteorological Department (IMD), 1999]. Though there are many adaptable parameters used in extra-tropics for hail warning, warning based on reflectivity factor is widely used both in tropics and extra-tropics. It is based on the premise that the presence of hail would enhance the reflectivity factor above freezing level owing to their size. The HW product needs radar reflectivity data from a volume scan. Two thresholds above the lower hail level (normally this level is often considered as freezing level) are set to identify the probable (40 dBZ and more) and most probable (55 dBZ) hail occurrence. These thresholds are adaptable depending on local conditions and weather events. However, it is assumed that even in heavy rains without hail the dBZ values above freezing level would not exceed these threshold values. In the present set up at DWR, Chennai, the Hail Warning product analyses reflectivity data for areas of probable or very probable hail occurrence. Such areas are indicated by (warning) coloured areas, which can be under-laid by reflectivity data. In case of probable hail occurrence, the user is alerted by audio and visual alarms. A sample display of hail warning is shown in Fig. 10 (a). It may be mentioned here that small hail stones were reported by electronic and print media around 0900 UTC at 10-15 km west of DWR, Chennai in the areas marked as hail very probable. As already stated, though the chances of hail storm in coastal Tamilnadu and coastal Andhra Pradesh are very less, with the available products and flexibility to adapt suitable parameters, it will be possible to develop suitable algorithm for hail warning in the radio horizon of Chennai, in the near future, if authentic reports of hail occurrence are received.

(b) *Warning (WRN)*

The warning product is a second level product. This means that the warning product depends on other products (also called first level products) and not on polar raw data. The idea is to take one or more first level products and to search for segments that match the conditions defined in the PDF worksheet. The base product is read and all pixels that match the threshold condition are set. If more than one condition is defined, all pixels satisfying one of the conditions are set. In a circular region (diameter of this circle is an adaptable parameter) around each pixel (set or reset) the number of set neighbours is evaluated. If a sufficient number of neighbours is set (fill percentage is an adaptable parameter) then the pixel is set otherwise it is reset (set to no data status). All neighbours in a circular region around a set pixel are also set. The effect is that groups of loosely connected pixels, close to each other, become connected and form segments. All set pixels that are neighbours to a segment are combined to that segment. The definition of neighbourhood is that one pixel is above, below, to the left or to the right of the segment. If the number of segments exceed the internally set upper limit then only the largest segments are kept. If more than one condition is defined, then segments are generated for each condition and combined according to the logical operator chosen by the user. Finally segments are displayed in symbol, colour, and or colour contour. Acoustic warning

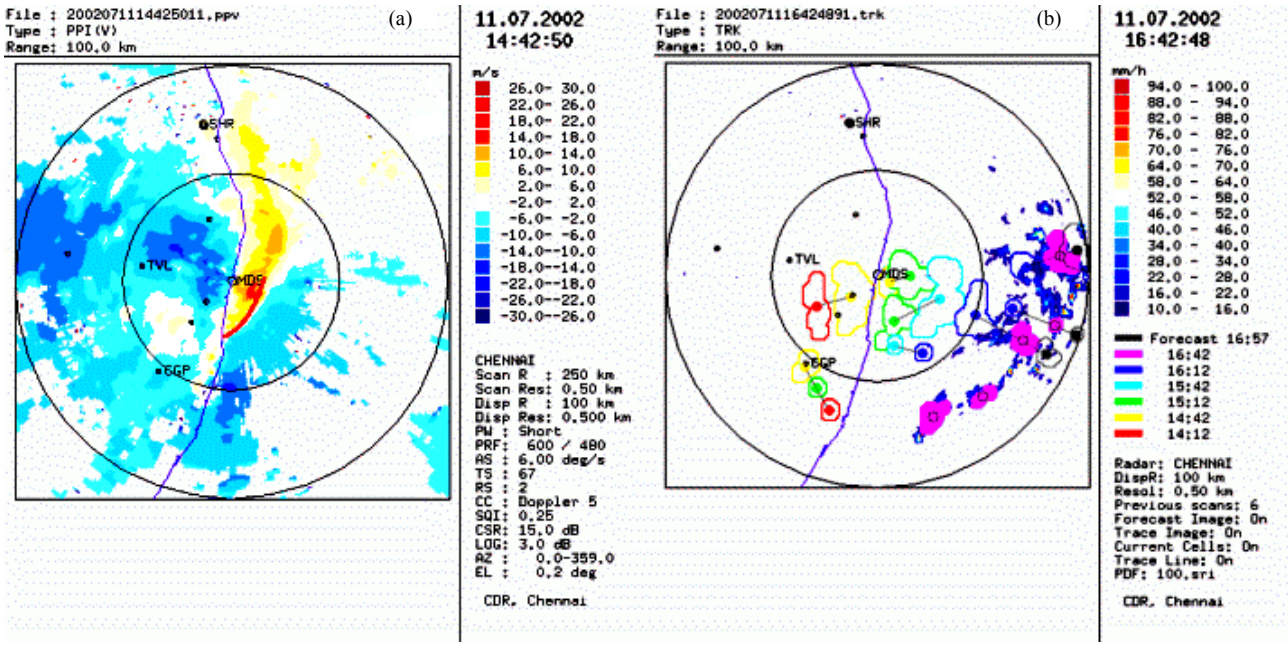

Figs. 11 (a&b). (a) Display of Gust front product (gust front is marked as a parabola in thick line) and (b) Tracking product showing track of rain event and its probable prediction

and or visual warning options also have been provided. Fig. 10(b) shows a typical display of warning product when thunderstorm is probable with reflectivity factor exceeding 50 dBZ at 0.2° elevation. The advantage of this product is that once the warning conditions are set depending on the operational requirement, the automatic generation of warning product alerts the user through audio/visual means and hence this product has tremendous potential for nowcasting sever weather events.

(c) *Tracking product (TRK)*

The tracking product is a second level product using already generated product(s) as input. Depending on the user defined input parameters such as the threshold value of dBZ or radial velocity or rain rate etc. with relevant relational operators (<, >, =, ≤, ≥), diameter and the minimum % filling of the individual cells with the criteria defined, it takes other product(s) as input and looks for cells that match the conditions defined in the PDF sheet. Some characteristic values are calculated for every cell and saved in a display list. Upto this stage, the logic of generating a tracking product is very similar to that of a warning product. The tracking algorithm takes subsequent display lists as input and tries to couple the cells in these lists. This is an iterative process, *i.e.* if there are uncoupled cells after the first run then the algorithm starts again with less restrictive conditions until all acceptable couplings have been found. The last step is a forecast about the future movement of the cells in the latest scan [Fig. 11(b)]. Cells are assumed to move on with unchanged speed and direction. Speed and direction are either calculated from the subsequent positions of coupled cells or, if there is no coupling, from the overall movement of all cells. During normal operation, the RAINBOW application software generates base products from raw data sets coming directly from the radar or from archived data. After every generation of a base product, a check is done as to whether tracking is active and whether all base products are available with the same time stamp. If all base products are available the tracking starts and generates a tracking image that is sent to the Display Manager.

4.6. *Phenomena Detection and Aviation products*

(a) *Gust Front Detection (GUF)*

The cold air transported by downdraft from a thunderstorm forms a diverging pool at the surface. A microscale cold front formed by the leading edge of this

pool is called gust front. Sudden drop in temperature and strong shifting winds are the immediate impact of the onset and movement of a gust front over a place. Low level convergence is associated with the propagation of gust front. Hence new thunderstorm cell formation usually occurs on the flanks of the old cell. In other words, gust front marks the leading edge of the cold air from the downdraft which lifts the warm moist air adjacent to earth surface to the level of free convection. Gust fronts often appear as thin line echoes (with radar reflectivity factor less than 20 dBZ, typically) on the display. The reflectivity of this order is due to lifting of insects, dust and aerosols into the atmosphere and concentration of birds [to catch their prey (insects) in the front. Gust fronts move to a greater distance ahead of the parent storm and are, at times, physically identified in the radar displays even after the dissipation of the parent storm (Burgess and Lemon, 1990; Rinehart, 1999]. Gust fronts are small lengthy regions (a few tens of km) and last for a few tens of minutes to an hour. The presence of gust front is very significant to aviation on two aspects; one, it indicates the presence of a thunderstorm in a nearby location and two, for taking a quick decision on the use of proper runway for safe aircraft operations when the time of arrival of a gust front and the direction from which it is approaching is known before hand. Gust front is itself an aviation hazard because of wind shear.

The Gust front algorithm calculates a nine ordinate sliding average for each bin in radial direction to smooth the radial velocity data. A search is made, ray by ray, in the radial direction for regions with decreasing velocities. Subsequent range bins with decreasing velocities in each ray are grouped to form a vector. Slopes of the range bins within the vector and the slope of the individual vector are worked out. A vector will be selected to form part of a gust front when its velocity slope exceeds 0.5 $ms^{-1}km^{-1}$ and its volume flow exceeds 30 ms^{-1} km and slope of velocity exceeds 0.65 ms^{-1} km^{-1} between subsequent bins within a vector or the volume flow exceeds 100 ms^{-1} km (Smith *et al*., 1989; Eilts *et al*., 1991). Selected vectors that satisfy conditions stipulated in the gust front algorithm are combined to form segment(s) through an iterative process. A parabola is matched to each of these regions by the method of least square fit. These parabolas are displayed on a product selected by the user to mark the location of the gust front. A typical gust front display (parabolic curve marked in thick line) is shown in Fig. 11(a) with PPI(V) as its underlay.

(b) *Layer turbulence (LTB)*

If all the samples within a resolution volume move with the same speed either towards or away from the radar, then the reflected power from such samples would have a single frequency and hence the spectral line would approach infinitesimal width. However, in turbulent conditions, each scatterer in sample volume will move in different directions and with different speed relative to the radar and therefore we get a spectrum of frequencies within the resolution volume. The spectral width will increase with the turbulence since the returned power will spread over a range of frequencies. As such, the Doppler Spectrum Width may throw some light on the prevalence of turbulence. However, it should also be remembered that several other factors, *viz*., antenna motion, differential fall of hydrometeors and wind shear also contribute to increased spectrum width (Doviak and Zrnic, 1984; Rinehart, 1999). Sato and Woodman (1982) established the presence of pronounced shear and enhanced spectrum width in the layered structure of turbulence. The LTB product takes a polar volume data set with spectral width data as input. The polar volume is converted to a Cartesian volume and a maximum display (top projection) of spectral width values is generated. A sample display of LTB in the layer between 0.1 and 1.0 km above ground level is shown in Fig. 12. Spectrum width in excess of 4.0 $ms^{-1}km^{-1}$ is considered to be associated with moderate turbulence (Rinehart, 1999).

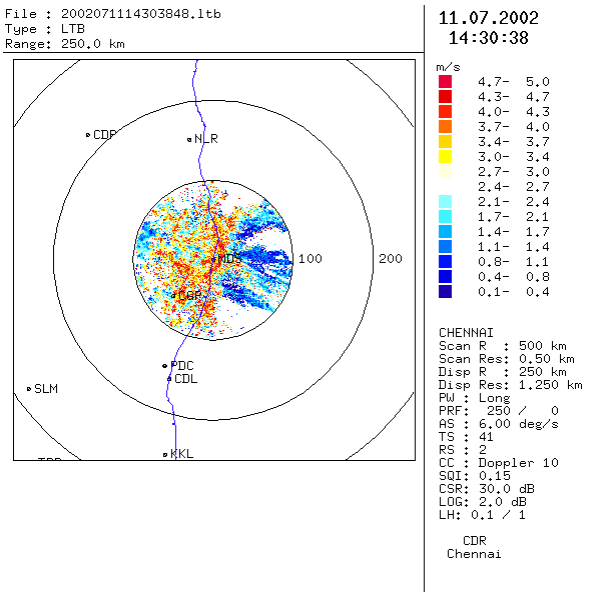

Fig. 12. Product showing layer turbulence between 0.1 and 1.0 km above ground level

5. Summary

As far as the numerous user friendly products are concerned DWR is a quantum jump from the conventional

radar. Though the products described in section 3.2 have been tested and are currently used elsewhere (in NEXRAD, German weather service, Royal Netherlands Meteorological Institute, Swiss weather services etc.), they are yet to be validated in India for the tropical weather situations. Attempts have been made at DWR, Chennai to validate some of the products since November 2001. Validation of the remaining products and operationalisation of products for its utility in realtime nowcasting local/aviation weather are being done at present. It is hoped that the continued research on some of the weather systems tracked since November 2001 will pave way for augmenting the weather forecasting capability and understanding the atmospheric processes.

Acknowledgements

The authors are thankful to the Director General of Meteorology, India Meteorological Department, New Delhi for extending the DWR facility at Chennai. Enthusiastic support extended by the staff and officers of DWR, Chennai is gratefully acknowledged. Thanks are also due to the referee for meticulously going through the manuscript and for his constructive comments and suggestions to improve the quality of the paper.

References

Andrieu, H. and Creutin, J. D., 1995, "Identification of vertical profiles of radar reflectivities for hydrological applications using an inverse method - Part I : Formulation", *J. Appl. Meteor*., **34**, 225-239.

Atlas, D., 1990, "Radar in Meteorology : Battan memorial and 40th anniversary radar meteorology conf.", ed. : David Atlas, *Amer. Met. Soc.,* Boston, p806.

Battan, L. J., 1973, "Radar observation of the atmosphere", University of Chicago press, Chicago, p324.

Battan, L. J., 1977, "Rain resulting from melting ice particles", *J. Appl. Meteor.*, **16**, 595-604.

Bear, V. E., 1991, "The transition from the present radar dissemination system to the NEXRAD information dissemination service (NIDS)", *Bull. Amer. Met. Soc.*, **72**, 1, 29-33.

Browning, K. A. and Wexler, R., 1968, "A determination of kinematic properties of wind field using Doppler radar", *J. Appl. Met*., **7**, 105-113.

Burgess, D. W. and Lemon, L. R., 1990, "Severe thunderstorm and detection by radar", in : Radar in Meteorology, ed. David Atlas, *Amer. Met. Soc.*, Boston, 619-647.

Crum, T. D. and Alberty, R. L., 1993, "The WSR-88D and WSR-88D operational support facility", *Bull. Amer. Soc*., **74**, 1669-1687.

Douglas, R. H., 1964, "Hail size distribution", Proc. 11th weather radar Conf., *Amer. Met. Soc.,* Boston, 146-149.

Doviak, R. J. and Zrnic, D. S., 1984, "Doppler radar and weather observations, Academic Press", London, p458.

Doviak, R. J. and Zrnic, D. S., 1993, "Doppler radar and weather observations, 2nd ed., Academic press, London, p562.

Eilts, M. D., Olson, S., Stumpf, G., Hermes, L., Abrevaya, A., Culbert, J., Thomas, K., Hondi, K. and Klingle-Wilson, D., 1991, "An improved gust front detection algorithm for the TDWR", Preprints. 4th international conference on aviation weather systems, 24-26 June 1991, Paris, J37-J42.

Heiss, W. H., McGraw, D. L. and Dale Sirmans, 1990, "Nexrad : Next generation weather radar (WSR-88D)", *Microwave Journal*, Jan 1990.

Huff, F. A., 1970, "Sampling errors in measurement of mean precipitation", *J. Appl. Meteorol*., **9**, 35-44.

India Meteorological Department, 1999, "Climatological tables of observatories in India", 1951-1980, 5th ed., IMD, New Delhi, 443-444.

Keeler, R. J. and Passarelli, R. E., 1990, "Signal processing for atmospheric radars", in : Radar in meteorology, ed. David Atlas, *Amer. Met. Soc.,* Boston, 199-229.

Klazura, G. E. and Imy, D. A., 1993, "A description of the initial set of analysis products available from the NEXRAD WSR-88D system", *Bull. Amer. Soc*., **74**, 1293-1311.

Lhermitte, R. M. and Atlas, D., 1961, "Precipitation motion by pulse Doppler radar", Pre-prints 9th radar meteorology Conf., Kansas city, *Amer. Met. Soc*., Boston, Massachusetts, 218-223.

Marshall, J. S. and Palmer, W. McK., 1948, "The distribution of raindrops with size", *J. Meteor.*, **5**, 165-166.

Persson, P. O. G. and Andersson, T., 1987, "A Real Time System: Automatic wind field interpretation of Doppler radar wind components", Proc. Symp. Mesoscale Analysis and Forecasting, Vancouver, European Space Agency, **SP282**, 61-66.

Rinehart, R. E., 1999, "Radar for Meteorologists", 3rd ed., Rinehart Publications, N.D.58206 –6129, USA, p428.

Sato, T. and Woodman, R. F., 1982, "Fine altitude resolution observations of stratospheric turbulent layers by Arecibo 430 MHz radar", *J. Atmos. Sci*., **39**, 2546-2552.

Skolnik, M. I., 1970, "Radar Handbook", McGraw Hill Book Co., New York, Chap **14**, 1-32.

Smith, S. D., Witt, A., Eilts, M. D., Hermes, L. G., Klingle-Wilson, D., Olson, S. H. and Patrick Sanford, J., 1989, "Gust front detection algorithm for the terminal Doppler weather radar, Part I : Current status", Preprints. 3rd international conference on the aviation weather system, *Amer. Met. Soc*., 31-34.

Waldteufel, P. and Corbin, H., 1979, "On the Analysis of Single-Doppler Radar Data", *J. Appl. Met*., **18**, 532-542.

Annexure I

Hardware specifications of DWR, Chennai

Radome		Antenna	
Panel type	Epoxy-foam Sandwich	Reflector type	Prime focus feed
No. of panels	66	Polarisation	Linear, Horizontal
Shape of panels	Hexagonal/Pentagonal	Scan rate	0.16 – 6 RPM (1° /S to 36° /S)
Diameter	11.6 m	Beam width	1 degree
Attenuation	< 0.7 dB one-way at 10 mm/h	Gain	44.5 dBi
Side lobe degradation	<1dB	Dish diameter	8.5 m

Receiver

Analogue Part		Digital Part	
Type	Double super heterodyne	Band width	Z mode: 1MHz, V mode 0.5MHz
1ST Local Osc.(LO)	2400 MHz	A/D conversion	40 MHz, 12 bit
Second LO	465,466,467,468 MHz	Signal processing by	15 Fast DSP chips of 120 MFLOPs /sec each
Intermed. Freq (IF)	475, 10 MHZ	Simultaneous output	Z, V and W, 8 bit each
Noise figure	1.5 dB maximum	Range bin spacing	Minimum 75m
M D D S in LP	-114 dBm	No. of range gates	Maximum 2000
M D D S in SP	-112 dBm	Dynamic range	Better than 95 dB

Transmitter

Type	Klystron amplifier
Modulator type	Hard switched, solid state
Frequency	2875 to 2878 MHz
Peak pulse power	750 KW
Pulse width	2 μS in Long Pulse (LP), 1 μS in Short Pulse (SP)
Pulse repetition frequency (PRF)	250 to 550 Hz in LP and 250 to 1200 in SP

Note : MDDS – Minimum Digitally Detectable Signal

Annexure II

Typical scan strategy adopted in DWR, Chennai

Item	Scan strategy 1	Scan #2	Scan #3	Scan #4
Scan range (km)	250	250	500	250
Scan name	Dual PRF (Velocity unfolding)	250 km volume scan	Frequency agility…500km volume scan	Second trip recovery
Pulse repetition frequency (PRF)	600 / 480	600	300	1200
Range resolution (km)	0.5	0.5	1.0	0.5
Range sampling	2	2	2	1
Unambiguous velocity (with velocity unfolding) (m s^{-1})	62.58	15.64	7.82	31.29
Antenna speed (deg /sec)	6	9	9.0	9.16
Time sampling	80	67	33	131
Clutter to signal ratio (dB)	15.0	15.0	30.0	30
Log threshold (dB)	3.0	3.0	2.0	2.0
Signal quality index	0.25	0.25	0.25	0.25
Doppler clutter filter No.	5	4	10	5
No. of antenna elevation steps	12	12	7	1
Elevation angles (degrees)	0.2, 0.7, 1.3, 2.0, 2.7, 3.4, 4.0, 4.8, 5.9, 7.8, 11.2, 19.8	0.2,0.7,1.3,2.0, 2.7,3.4,4.0,4.8, 5.9, 7.8, 11.2, 19.8	0.2, 1.0, 2.0, 3.0, 4.0, 5.0, 6.0	0.2
Time taken for each volume scan (minutes)	12	8	4.7	1.5